Acta Mechanica Solida Sinica, Vol. 21, No. 4, August, 2008 ISSN 0894-9166
Published by AMSS Press, Wuhan, China. DOI: 10.1007/s10338-008-0832-3

ANALYSIS ON PSEUDO-STEADY INDENTATION CREEP

Hidenari Takagi[1⋆] **Ming Dao**[2] **Masami Fujiwara**[1]
([1] *Division of Applied Physics, College of Engineering, Nihon University, Fukushima, Japan*)
([2] *Department of Materials Science and Engineering, School of Engineering, Massachusetts Institute of Technology, Massachusetts, USA*)

Received 24 June 2008; revision received 19 July 2008

ABSTRACT Theoretical analysis and finite element (FE) simulation have been carried out for a constant specific load rate (CSLR) indentation creep test. Analytical results indicate that both the representative stress and the indentation strain rate become constant after a transient period. Moreover, the FE simulation reveals that both the contours of equivalent stress and equivalent plastic strain rate underneath the indenter evolve with geometrical self-similarity. This suggests that pseudo-steady indentation creep occurs in the region beneath the indenter. The representative points in the region are defined as the ones with the equivalent stress equal to the representative stress. In addition, it is revealed that the proportionality between indentation strain rate and equivalent plastic strain rate holds at the representative points during the pseudo-steady indentation creep of a power law material. A control volume (CV) beneath the indenter, which governs the indenter velocity, is identified. The size of the CV at the indented surface is approximately 2.5 times the size of the impression. The stress exponent for creep can be obtained from the pseudo-steady indentation creep data. These results demonstrate that the CSLR testing technique can be used to evaluate creep parameters with the same accuracy as conventional uniaxial creep tests.

KEY WORDS indentation creep, finite element method, conical indenter, geometrical self-similarity, pseudo-steady state, control volume, stress exponent

I. INTRODUCTION

The instrumented indentation test can be used for evaluating mechanical properties within a selected local region of a small specimen at room temperature or high temperature. However, nanoindenters normally can only be used at the room temperature, due to thermal drift as well as other complications resulted from elevated temperatures. To overcome this limitation, Fujiwara[1] developed a microindenter which can be performed at 1000 K and even above.

Takagi et al.[2,3] employed the microindenter for constant-load indentation (CLI) tests and indention-load jump tests using a conical indenter. They also evaluated creep parameters such as stress exponent, activation energy for creep, and so on. The creep parameters obtained from these CLI tests agreed well with those obtained from conventional tensile creep tests.

In a CLI test, the equivalent stress and equivalent plastic strain rate underneath the indenter decrease gradually as the indentation creep develops. Therefore, it is difficult to evaluate creep parameters for a steady state in which dynamic recovery does not occur sufficiently during CLI testing. When the geometrically self-similar contours of equivalent stress and equivalent plastic strain rate evolve during a constant specific load rate (CSLR) indentation creep test, the indenter tip is surrounded by a practically equivalent mechanical condition with respect to the self-similarly expanding geometry. In other words,

the indenter tip can continuously detect a constant (steady-state) deformation-induced representative stress and a steady-state indentation strain rate. We call such a deformation behavior pseudo-steady indentation creep.

Using theoretical analysis and finite element (FE) simulation, this study reveals that pseudo-steady indentation creep occurs in a region underneath the indenter when an indentation creep test is carried out under a specified load condition. To this end, we attempt to investigate the following aspects:

– Establishing a governing constitutive equation for a constant specific load rate (CSLR) test;
– Confirming the geometrical self-similarity through FE simulations of the CSLR test regarding the expanding equivalent stress field and equivalent plastic strain rate field beneath the indenter;
– Defining the representative points in the region of indentation creep, and establishing the relationship between equivalent plastic strain rate and indentation strain rate at these points; and
– Identifying an indentation creep control volume (CV) underneath the indenter, which governs the indenter velocity.

II. CONSTITUTIVE EQUATION OF PSEUDO-STEADY INDENTATION CREEP

When the contours of equivalent plastic strain expand with geometrical self-similarity, the indentation strain rate $\dot{\varepsilon}$ can be defined as[4]:

$$\dot{\varepsilon} = \frac{\dot{u}}{u} \tag{1}$$

where u is the indenter displacement, and $\dot{u}$ is the indenter velocity. The representative stress σ can be defined by

$$\sigma = C_1 p \cong \frac{F}{3\pi u^2 \tan^2\theta} \tag{2}$$

where C_1 is taken as $1/3$[5], p the indentation pressure, F the indentation load, and θ the included half apex-angle of the conical indenter and equals 68 degrees for the indenter used in the present study. The representative points in the region of indentation creep can be defined as points that have equivalent stress $\bar{\sigma}$ with the same value as the above-mentioned σ. For compatibility, the equivalent plastic strain rate $\dot{\bar{\varepsilon}}$ at these points can be described as

$$\dot{\bar{\varepsilon}} = C_2 \dot{\varepsilon} \tag{3}$$

where C_2 is a dimensionless constant and equals 3.6^{-1} with the case for the stress exponent: $n = 3.0$ and $\theta = 68$ degrees, which will be discussed in §4.3.

It is assumed that the following power-law creep relationship holds between $\bar{\sigma}$ and $\dot{\bar{\varepsilon}}$

$$\dot{\bar{\varepsilon}} = A_1 \left(\frac{\bar{\sigma}}{E}\right)^n \tag{4}$$

where A_1 is a temperature-dependent constant, E the Young's modulus, and n the stress exponent for creep. Combining Eq.(1) to Eq.(4), the following constitutive equation of indentation creep can be obtained

$$\dot{\varepsilon} = A_2 \left(\frac{\sigma}{E}\right)^n = A_3 \left(\frac{F}{Eu^2}\right)^n \tag{5}$$

where $A_2 = A_1/C_2$ and $A_3 = A_1(3\pi \tan^2\theta)^{-n}/C_2$.

In the CSLR test, we consider the case where $\dot{F}/F = \text{constant}$[6]. In this case, the loading function is described as follows:

$$F = F_0 \exp(\lambda t) \tag{6}$$

where F_0 is the initial load, λ a constant, and t the loading time. Substituting Eq.(6) into Eq.(5) and then integrating the resulting equation, we obtain

$$u(t) = \sqrt{\frac{F_0}{E}\left\{\frac{2A_3}{\lambda}\left[\exp(\lambda n t) - 1\right]\right\}^{1/n}} \tag{7}$$

Based on Eqs.(2), (6) and (7), the representative stress σ can be obtained

$$\sigma = E\left\{\frac{\lambda}{2A_2}\left[1 - \exp(-\lambda n t)\right]^{-1}\right\}^{1/n} \tag{8}$$

The indentation strain rate $\dot{\varepsilon}$ can be expressed as

$$\dot{\varepsilon} = \frac{\mathrm{d}\ln u}{\mathrm{d}t} = \frac{\lambda}{2}\left[\frac{1}{1-\exp(-\lambda n t)}\right] \tag{9}$$

When $t \gg 1/(\lambda n)$ in Eqs.(8) and (9), σ and $\dot{\varepsilon}$ become constant as follows:

$$\sigma \cong E\left(\frac{\lambda}{2A_2}\right)^{1/n} \equiv \sigma_s = \text{const} \tag{10}$$

$$\dot{\varepsilon} \cong \frac{\lambda}{2} \equiv \dot{\varepsilon}_s = \text{const} \tag{11}$$

Using σ_s and $\dot{\varepsilon}_s$, the constitutive equation of pseudo-steady indentation creep can be obtained as

$$\dot{\varepsilon}_s = A_2\left(\frac{\sigma_s}{E}\right)^n \tag{12}$$

Therefore, the stress exponent n for creep can be evaluated by

$$n = \frac{\partial \ln \dot{\varepsilon}_s}{\partial \ln(\sigma_s/E)} \tag{13}$$

III. COMPUTATIONAL MODEL

Figure 1 shows schematically the FE model. The conical indenter is assumed rigid with an apex angle $2\theta = 136°$. The indented material is taken as elastoplastic and modeled with four-node bilinear axisymmetric quadrilateral elements. Each element is set to conform to the power-law creep equation: $\dot{\bar{\varepsilon}} = A_1(\bar{\sigma}/E)^{n'}$, where $A_1 = 54.0 \times 10^6$ s^{-1}, $E = 37.8 \times 10^3$ MPa, and $n' = 3.0$. Numerical simulations on the CSLR test were carried out using a general-purpose finite-element package, ABAQUS (SIMULIA Inc.), and a self-made user subroutine. The indentation loading was controlled by $F = F_0 \exp(\lambda t)$ with $F_0 = 0.294$ N and $\lambda = 0.5\times10^{-3} - 6\times10^{-3}\ \mathrm{s}^{-1}$. The FE simulations were stopped at the maximum indentation load of 2.94 N because further deformation might be influenced by the boundary conditions. More details on the computational model set-up can be found elsewhere[2, 7].

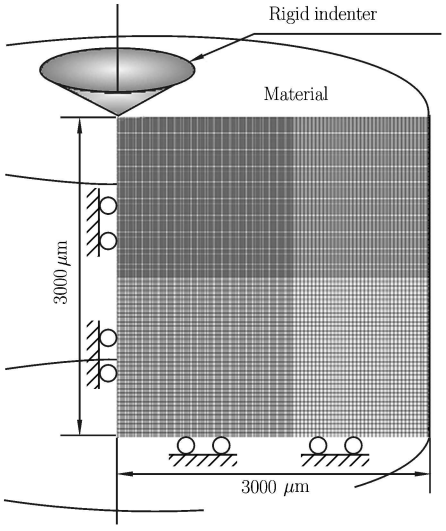

Fig. 1: A schematic FE model.

IV. RESULTS AND DISCUSSIONS

4.1. Indentation Creep Curve

The solid lines in Fig.2 show the time dependence of the indenter displacement u obtained from Eq.(7), which increases very quickly for large λ. The computational results (marked with circles) agree well with the theoretical analysis.

Figure 3 shows the time dependence of the representative stress σ. Obviously, the computational results (marked with circles) agree well with the theoretical analysis (shown by solid lines) obtained from Eq.(8), too. It is clear that σ decreases very rapidly at the initial loading stage, and then gradually becomes constant after a certain loading duration. For example, when $\lambda = 1 \times 10^{-3}$ s^{-1}, the

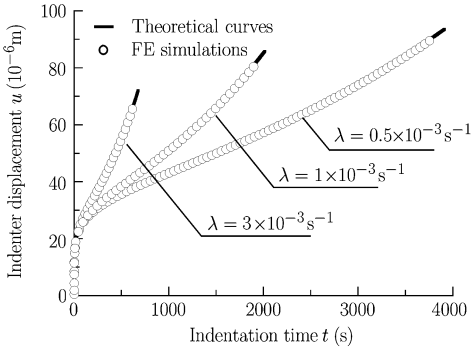

Fig. 2: Time dependence of indenter displacement.

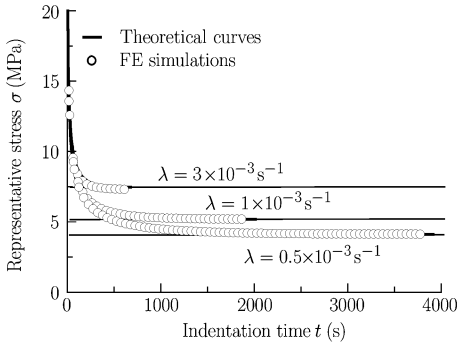

Fig. 3. Time dependence of representative stress.

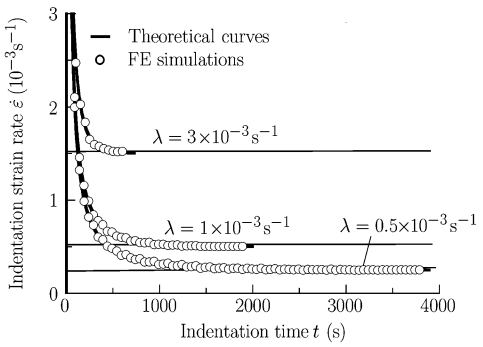

Fig. 4. Time dependence of indentation strain rate.

moment for that σ becomes constant is about 1000 s. This agrees well with the result expected from using Eq.(10).

Figure 4 shows the time-dependence of the indentation strain rate $\dot{\varepsilon}$. Numerical results (marked with circles) agree well with the theoretical analysis (shown by solid lines) obtained from Eq.(9). $\dot{\varepsilon}$ decreases as indentation creep proceeds at the initial loading stage, and then becomes constant after a certain period, similar as σ in Fig. 3. This agrees well with Eq.(11).

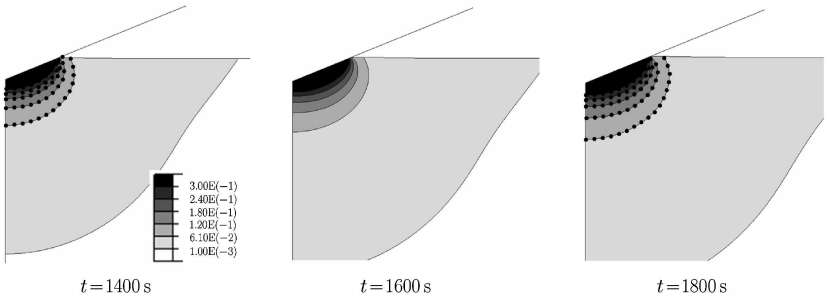

Fig. 5. Time dependence of the contours of equivalent plastic strain.

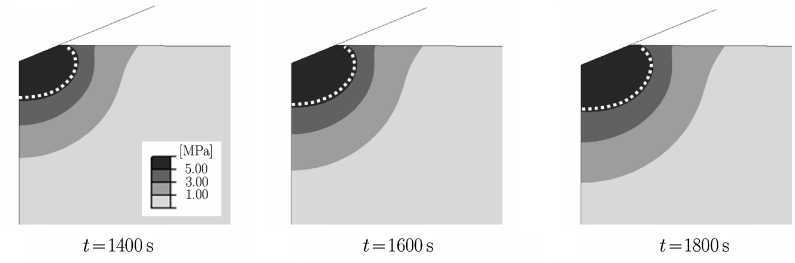

(a) Equivalent stress

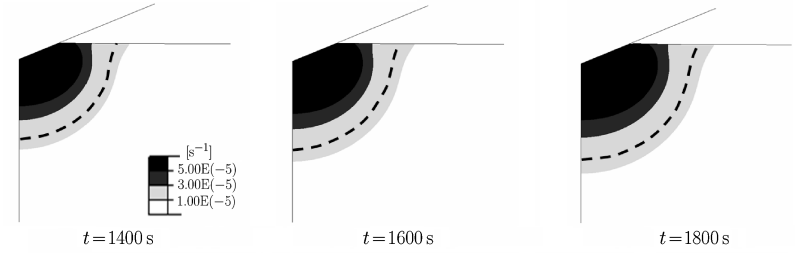

(b) Equivalent plastic strain rate

Fig. 6. Time dependence of the contours of (a) equivalent stress and (b) equivalent plastic strain rate.

The above results show that when a load is applied as in Eq.(6), σ and $\dot{\varepsilon}$ can maintain constant values of σ_s and $\dot{\varepsilon}_s$ after a transient period. This also implies that the stress exponent for creep can be evaluated by Eq.(13).

4.2. Pseudo-steady Indentation Creep

Figure 5 shows the contours of equivalent plastic strain obtained from FE simulation at $\lambda = 1 \times 10^{-3}$ s^{-1}. Each contour is drawn based on the data in Figs.3 and 4. Indenter displacement is 62.9 μm at 1400 s, 69.6 μm at 1600 s, and 76.9 μm at 1800 s. By enlarging and reducing the contour of 1600 s with the scale of each indenter displacement, the enlarged and reduced contours (shown by dotted lines) can be superimposed with the original contours of 1400 s and 1800 s. The dotted lines correspond well to the original contours, which indicates that the contours of equivalent plastic strain in the region immediately beneath the indenter expand self-similarly during indentation creep. Therefore, the indentation strain rate can be described by Eq.(1).

Figure 6 shows (a) the contours of equivalent stress, and (b) the contours of equivalent plastic strain rate, when $\lambda = 1 \times 10^{-3}$ s^{-1}. It is confirmed in the same way as in Fig.5 that all contours expand self-similarly. This indicates that pseudo-steady indentation creep occurs in the region beneath the indenter, as the indenter tip is surrounded by self-similar stress and strain fields as indentation creep develops. This result implies that the indenter tip can continuously detect the constant (i.e. steady state) deformation-induced representative stress and the steady-state indentation strain rate.

Figure 7 logarithmically shows $\dot{\varepsilon}_s$ versus σ_s/E. According to Eq.(13), the slope of the straight lines corresponds to the stress exponent n for creep, which can be obtained there as 3.0. This suggests that the stress exponent can be correctly extracted using σ_s and $\dot{\varepsilon}_s$ calculated with the indenter displacement.

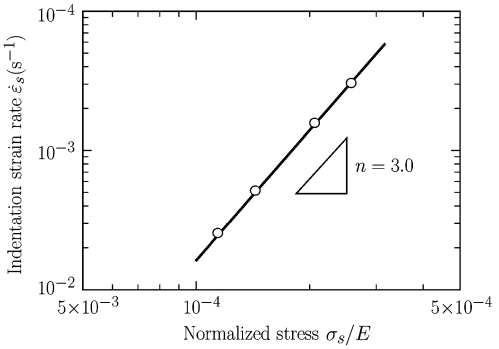

Fig. 7: Logarithmic plots of $\dot{\varepsilon}_s$ versus σ_s/E based on FE simulation results.

4.3. Relationship between Indentation Strain Rate and Equivalent Plastic Strain Rate

The relationship between indentation strain rate $\dot{\varepsilon}$ and equivalent plastic strain rate $\dot{\bar{\varepsilon}}$ has not been systematically investigated in the literature so far. To study this relationship, we begin with the case for $\theta = 68°$ and $n = 3.0$. The representative stress can be defined as $\sigma = C_1 p$ using the appropriate constraint factor ($C_1 \cong 1/3$). The representative points in the region beneath the indenter are defined as the ones with the equivalent stress $\bar{\sigma}$ equal to the representative stress σ_s.

In Fig.6(a), the contours of $\sigma_s = \bar{\sigma} = 5.2$ MPa, which are on the representative points, are denoted by the white dotted lines at $\lambda = 1 \times 10^{-3}$ s^{-1}. $\dot{\bar{\varepsilon}}$ at the representative points is about 1.43×10^{-4} s^{-1} at the steady state. From Fig.4, $\dot{\varepsilon}_s$ is equal to 0.5×10^{-3} s^{-1}. Thus, a relationship of $\dot{\bar{\varepsilon}} = C_2 \dot{\varepsilon}_s = 3.5^{-1} \dot{\varepsilon}_s$ can be identified. When $\lambda = 0.5 \times 10^{-3} - 6 \times 10^{-3}$ s^{-1}, we have $C_2 = 1/3.5 - 1/3.7$, and consequently the average C_2 value in this testing condition is approximately 1/3.6.

4.4. Determination of the Control Volume

It is estimated that the region beneath the indenter where equivalent plastic strain rate is 1/10 or less of indention strain rate would not have a substantial effect on the indenter velocity. In this case, the control volume (CV) in pseudo-steady indentation creep can be defined as $\dot{\bar{\varepsilon}}_{CV} \geq \dot{\varepsilon}_s/(3.6 \times 10) = \lambda/72$, where the indenter velocity is primarily controlled by the deformation in the CV.

In Fig.6(b), the outline of the CV is designated by the black dashed lines. The size of the CV at the indented surface is about 2.5 times the size of the impression. During a pseudo-steady indentation creep, the surface of the CV expands self-similarly. As shown in Fig.6(b), equivalent plastic strain rate rapidly decreases to almost zero outside the CV, which indicates that the above definition of $\dot{\bar{\varepsilon}}_{CV} \geq \lambda/72$ is appropriate.

V. CONCLUSIONS

(1) Theoretical and computational results show that representative stress and indentation strain rate become constant after a transient period in CSLR tests.

(2) Both the contours of equivalent stress and equivalent plastic strain rate underneath the indenter expand self-similarly. This indicates that a pseudo-steady indentation creep occurs in the region beneath the indenter.

(3) The representative points are defined as the points that have equivalent stress of $\bar{\sigma} \cong p/3$. It is found that the relationship $\dot{\bar{\varepsilon}} = \dot{\varepsilon}_s/3.6$ holds at the representative points during pseudo-steady indentation creep with $n = 3.0$ and $\theta = 68°$.

(4) The control volume (CV) is defined as the volume underneath the indenter, which governs the indenter velocity. The size of CV at the indented surface is approximately 2.5 times the size of the indentation impression.

(5) The above results demonstrate that the CSLR testing technique can be used to evaluate creep properties with the same accuracy as conventional uniaxial creep tests.

References

[1] Fujiwara,M., Characterization of mechanical properties in materials through instrumented indentation. *Journal of Japan Institute of Light Metals*, 2002, 52: 282-290.

[2] Takagi,H., Dao,M., Fujiwara,M. and Otsuka.M., Experimental and computational creep characterization of Al-Mg solid-solution alloy through instrumented indentation. *Philosophical Magazine*, 2003, 83: 3959-3976.

[3] Takagi,H., Dao,M., Fujiwara,M. and Otsuka,M., Creep characterization of aluminum-magnesium solid-solution alloy through self-similar microindentation. *Materials Transact*, 2006, 47: 2006-2014.

[4] Pollock,H.M., Maugis,D. and Barquins,M., Microindentation Techniques in Materials Science and Engineering. Blau,P.J. and Lawn,B.R. eds, (ASTM, Philadelphia, 1986): 47-71.

[5] Tabor,D., The Hardness of Metals. Oxford University Press, 1951.

[6] Cheng,Y.T. and Cheng,C.M., Scaling relationships in indentation of power-law creep solids using self-similar indenters. *Philosophical Magazine Letter*, 2001, 81: 9-16.

[7] Takagi,H. and Fujiwara,M., Creep characterization of power-law materials through pseudo-steady indentation tests. *Materials Science Forum*, 2007, 561-565: 2063-2066.